New Materials and Structures for Photovoltaics

ALEX ZUNGER

National Renewable Energy Laboratory, Golden, CO 84001

S. WAGNER

Department of Electrical Engineering, Princeton University, Princeton, NJ 08544

P. M. PETROFF

Materials Department, University of California, Santa Barbara, CA 93106

Despite the fact that over the years crystal chemists have discovered numerous semiconducting substances, and that modern epitaxial growth techniques are able to produce many novel atomic-scale architectures, current electronic and opto-electronic technologies are based but on a handful of ~10 traditional semiconductor core materials. This paper surveys a number of yet-unexploited classes of semiconductors, pointing to the much-needed research in screening, growing, and characterizing promising members of these classes. In light of the unmanageably large number of a-priori possibilities, we emphasize the role that structural chemistry and modern computer-aided design must play in screening potentially important candidates. The basic classes of materials discussed here include nontraditional alloys, such as non-isovalent and heterostructural semiconductors, materials at reduced dimensionality, including superlattices, zeolite-caged nanostructures and organic semiconductors, spontaneously ordered alloys, interstitial semiconductors, filled tetrahedral structures, ordered vacancy compounds, and compounds based on d and f electron elements. A collaborative effort among material predictor, material grower, and material characterizer holds the promise for a successful identification of new and exciting systems.

Key words: New materials, new structures, photovoltaics

INTRODUCTION

Time Scales for Research on the Generation of Bulk Power by Photovoltaics

Any discussion of directions and ideas for photovoltaic (PV) research must begin by specifying the time scale over which this research should come to fruition. The time scale for PV research, including very fundamental work, can legitimately range from near-immediate to 30 years and more. Photovoltaic manufacturers are producing now for many niche applications, which include applications by electric utilities. Doing research that helps these manufacturers is important, because they constitute a new industry, and because later on the experience gained with niche systems will be valuable for bulk power producers. Bulk power generation by PV in a volume that can be felt by large utilities is 20 to 30 years away. Although solid-state devices have short turnaround times in the laboratory and in manufacturing, electric utilities must test new systems for 10, 20, or 30 years for gaining the engineering experience needed for the planning and reliable integration of many such systems. An even longer time scale is set by environmentalism. Environmentalism is establishing its political power in the industrialized countries. The environmental agenda will be pushed for generations to come. The agenda will include the full exploitation of renewable energy. We can safely assume that even Utopian environmental ideas will come to pass, just as the Utopian ideas of late 19th century social democrats have become the foundation of the social contract in the democratic industrial countries of the late 20th century. The environmental agenda is placing a time scale of 100 years on PV, and encourages us to

(Received August 1, 1992)

take seriously far-out concepts like Kuwano's Genesis—a global network of PV power plants and superconducting transmission lines.

The terrestrial photovoltaic programs were begotten by the oil crises of the 1970s. Brought on by the sense of urgency of that period, most PV research and development programs understandably suffer from the birth defect of a short-term outlook. This sense of urgency acted to discourage unconventional ideas. Instead, many projects simply followed up concepts developed and demonstrated elsewhere. It is clear that soon-to-use technology must be developed, and that its development will continue to consume the majority of the available R&D budget. But forever we must keep in mind that in one sense we have very much time available, and that one of our obligations is to explore every idea that could lead to solar driven power production and storage.

Desired Properties of Photovoltaic Semiconductors

A number of properties are required of candidate PV materials and device structures. Among the most essential are:

- strong light absorption over a wide spectral range. This property implies that a tunable band g a p is desirable. The absorption should also peak around 1.4 eV for optimal performance.
- a large luminescence yield, a low carrier recombination loss, and efficient carrier collection efficiency are prerequisites for the new materials and structures,
- for lower cost, the structures should be of the thin film types with a long optical path to promote photon recycling,
- for space applications or a hard radiation environment, they should be radiation resistant, and
- the materials should enable stable metal contacts and should resist corrosion.

Of course the proposed structures should meet as many of these desired properties as possible. It is a difficult task to meet all of these at once, and we believe that a long range research effort will be necessary. For this reason, we will classify the research opportunities discussed here as "fundamental." Notice, however, that they could provide breakthroughs and spin-off application in a very short time scale. Obviously, in addition to undertaking an extensive research effort on the materials and structures, it will be wise to support a research effort on the device physics and device modeling for a number of the structures proposed in the next sections.

The Current Material Base of Photovoltaics: General Observations

Perhaps the most intriguing aspect of the spectacular success that semiconductor-based high technology has had in the past 50 years is the tiny number of species (core materials) on which these technologies are based. Even considering a broad range of semiconductor devices—transistors, computer chips, solid state lasers, detectors, solar cells, light-emitting diodes, etc.—one finds but an order ten basic semiconductors (all belonging to the same crystal type!), that enable these technologies. This is a strikingly narrow material base, considering the number of core materials that enable other technologies; e.g. the 10^3–10^5 species used in metallurgy, polymer technologies, biotech, and the pharmaceutical industry. The currently used "high tech" semiconductors also provide but a limited set of relevant materials properties, such as band gaps, lattice constants, effective masses, and mobilities. Of course, there are good historical reasons for this narrowness of material base, ranging from the stringent criteria that electronic devices place on material perfection and purity, to the natural human inertia associated with the large investments that have been made in the first semiconductor to work in a big way. Given, however, the remarkable progress in our ability to grow high-purity artificial structures, (even in defiance of conventional equilibrium thermodynamics), and the increasing need to diversify materials properties in new device architectures, one wonders whether time has come to take another, systematic look at enlarging the database of potentially useful electronic materials and structures. The obvious approach to this need is to use educated, phenomenological trial-and-error techniques that have brought us, among others, new superconductors, ferroelectrics, and quasicrystals. It is almost certain that a combination of such Edisonian approaches with a considerable amount of "guided luck" will continue to provide us with exciting new materials. There is, however, a possible complementary approach: use of solid state theory as a guide to selecting promising new materials. Indeed, while our theoretical understanding of the microscopic makings of ferroelectricity, quasicrystallinity, and unconventional superconductivity is yet to reach the state of a-priori material-predictive ability, our theoretical understanding of the structure versus function relationships underlying ideal semiconductivity is considerably more advanced. It is tempting at first to attribute this relative success to the important advances made in electronic structure theory[1]—effective-mass ideas, Landau's quasiparticles, the density-functional theory, pseudopotentials, total-energy methods, and large-scale simulation techniques. While this is, of course partially true, much of the current success in understanding property versus structure relationships in semiconductors reflects the dominance of single-particle physics over the more complex, explicit many-body, strongly correlated and cooperative phenomena underlying effects such as the multiplet structure of atoms, spin-glasses transitions, unusual superconductivity, and, to some extent, ferroelectricity.

This paper will outline some of the basic principles that permit design of new semiconductor crystal structures with prescribed band gaps. No attempt will be made to be all-inclusive. Our purpose is to describe the basic design principles as "food for thought" and

provide references for further detail.

The plan of this paper is as follows: we start (Band-Gap Tuning Through Formation of Random Alloys) by discussing how alloying of familiar materials can lead to structures with designed band gaps. We will emphasize in this section the lesser known research opportunities in the field of alloys, namely formation of non-isovalent and non-isostructural alloys. We will then move (Use of Reduced Dimensionality Structures for Photovoltaic Devices) to discuss the potential use of quantum structures in photovoltaics, including short-period superlattices (illustrating how band gaps could be tuned using layer orientation, strain, and interfacial roughness), lateral superlattices, free-standing as well as caged nanocrystalline structures and one-dimensional organic semiconductors. The next section (Band Gap Reduction Through Spontaneous Ordering of Semiconductor Alloys) discusses a novel phenomena of spontaneous ordering of otherwise random semiconductor alloys. This offers a new way of obtaining previously impossible band gap and mobility values from "ordinary" Group III-V and II-VI alloys. Band Gap Manipulations Through Direct Chemical Synthesis discusses direct chemical synthetic approaches to growth of nontraditional semiconductors (i.e. other than the century-old Group III-V and II-VI systems). We conclude with a sections on Biomimetric Structures and Structures With Separated Absorber and Transport Materials, and Summary.

BAND-GAP TUNING THROUGH FORMATION OF RANDOM ALLOYS

The simplest and by far the most widely used method for obtaining band gap values that are not provided by the repertoire of pure semiconductors is to form solid-solutions $A_{1-x}B_xC$ of the constituents AC and BC. The rich experience in this field[2-3] suggests that the physical property P (band gap, lattice constant, mixing-enthalpy, etc.) of random alloy is related to those of the constituents through the simple parabolic form

$$P(x) \cong [(1-x)\, P_{AC} + xP_{BC}] - b\, x\, (1-x) \qquad (1)$$

where b is a bowing parameter, and P_{AC} and P_{BC} are the values of the respective properties in pure AC and BC. Each optical transition (e.g. $\Gamma_{15v} \rightarrow \Gamma_{1c}$) has its own bowing parameter. This simple technique of physical mixing was used, for example, to obtain 1.9 eV photovoltaic materials such as GaInP and GaAlAs. There are two issues related with the use of Eq. 1 to obtain desired values of the band gap:

- one needs to know the bowing parameter b experimentally or theoretically, and
- one needs to know if AC and BC are miscible[2-4], or to make them miscible if they normally are not.

These two issues are discussed next.

Finding the Band Gap Bowing Parameter

To design a given band gap for an alloy between material AC and material BC, one needs to know the band gap of the constituents and the alloy's bowing parameter b (Eq. 1). This problem was solved experimentally for most isovalent alloys. We have tables of values of b for the common $(III\text{-}V)_{1-x}$ $(III\text{-}V)_x$ or $(II\text{-}VI)_{1-x}$ $(II\text{-}VI)_x$ alloys.[2-3] For values not measured, one can use theoretical estimates. The methods here range from simple pseudopotential-based virtual crystal models[5] to more quantitative first-principle methods.[6-8] Only the latter methods give reliable estimates for the bowing of the spin-orbit splitting.[7] What has been discovered in recent studies (e.g. Refs. 6–8) is that the bowing phenomenon is a result of the interplay between size-mismatch and charge transfer, so it cannot be simply calculated by a virtual crystal approach. The new theoretical methods[6-8] appear now capable of predicting the bowing even in not-yet-made alloys.

An example of such nontraditional alloys are the non-isovalent alloys, e.g. $(III\text{-}V)_{1-x}$ $(IV)_{2x}$, or $(III\text{-}V)_{1-x}$ $(II\text{-}VI)_x$ or $(II\text{-}VI)_{1-x}$ $(IV)_{2x}$. Measurements exist only for a few cases.[9] The theory of such systems shows that the non-isovalent alloys create natural donor and acceptor states that lead to charge-transfer and compensation. Two promising theoretical approaches were outlined recently,[10,11] but this area of research is still wide open. There are large number of combinations of non-isovalent alloys that can provide technologically interesting band gaps (even the direct-indirect crossover in the size-matched ZnS/Si alloys was never examined!).

Yet another opportunity for band gap tuning through alloy formation exists in the area of non-isovalent non-isostructural alloys. Examples include alloys between chalcopyrites and zincblende; e.g. $(CuInSe_2)_{1-x}$ $(ZnSe)_x$. Many such alloys were synthesized early on,[12] but there is little knowledge of their band gaps. Table I collects the available data on some of these alloys, indicating if solid solubility (SS) or limited solid solubility (LSS) exists. It would be important to calculate and measure the band lineup between such pairs as well as their optical properties.

Solubility of Binary Semiconductors

To benefit from the band gap bowing phenomena underlying Eq. 1, one has to be able to prepare a reasonably stable alloy. Melt and solution-growth[4] of semiconductor solid solutions shows that the alloy tends to phase-separate into its constituents below a miscibility gap temperature that increases with the relative size-mismatch $(a_{AC} - a_{BC})/\bar{a}$ of the constituents. Temperature-composition phase diagrams that describe this behavior are available experimentally for most common isovalent alloys.[2-4] They can now also be calculated reliably from first-principles[13-14] even for cases where no experimental data exist. Data is scarce for non-isovalent and non-isostructural alloys. Preliminary studies show that such phase dia-

Table I. Summary of Experimental Observations on Common-Anion Alloys of ABC_2 Chalcoppyrite with DC Zincblende Systems

ABC_2/DC	How Grown	What was measured	Ref.
$CuGaS_2$/ZnS	Chemical transport	SS: ZB, doping study	a
$CuGaSe_2$/ZnSe	Melt growth	SS: CH/ZB, lattice parameters	b
$CuGaTe_2$/ZnTe	Melt and anneal	LSS: CH/ZB, phase diagram, lattice parameters, opt. transmission and absorption	c
$CuInSe_2$/ZnSe	Melt growth	SS: CH/ZB, lattice parameters	d
	Melt growth	SS: CH/ZB, band gap (opt. absorption), carrier concentration (reflectivity), Raman	e
	Melt growth	Lattice parameters with vacancies	f
	Chemical transport	LSS: CH/ZB, band gap (opt. absorption), photoconductivity	g
$CuInTe_2$/ZnTe	Melt and anneal	LSS: CH/ZB, phase diagram, lattice parameters	h
	Melt and anneal	SS: CH/ZB, lattice parameters, band gap (opt. absorption)	i
	Melt and anneal	SS: CH/ZB, phase diagram	j
$CuInTe_2$/CdTe	Melt and anneal	SS: CH/ZB, lattice parameters, band gap (opt. absorption)	k
	Melt and anneal	SS: CH/ZB, phase diagram	l
$AgInTe_2$/ZnTe	Melt and anneal	LSS: CH/ZB, phase diagram, lattice parameters, band gap (opt. absorption)	i,m
$AgInTe_2$/CdTe	Melt and anneal	LSS:CH/ZB, lattice parameters, band gap (opt. absortion)	n
$AgInTe_2$/HgTe	Melt and anneal	LSS: CH/ZB, phase diagram, lattice parameters	o

SS = solid solutions; LSS = limited solid solutions; CH = chalcopyrite; ZB = zincblende.

grams may be calculated from first-principles; e.g. for $(CuInSe_2)_{1-x}(ZnSe)_x$[15] or $(GaAs)_{1-x}(Ge)_{2x}$,[11] but considerably more work is needed to examine this.

One manifestation of the power of modem crystal growth techniques is the ability to stabilize homogeneous solid solutions that we know thermodynamically to be unstable. This includes epitaxial growth techniques, enabling for example the growth of $(GaP)_{1-x}(GaSb)_x$ alloys whose components are totally immiscible in the bulk,[16] and beam-assisted growth techniques, enabling, for example, growth of $(GaAs)_{1-x}(Ge)_{2x}$ as a single-phase alloy[17] even though the bulk solubility is almost vanishing. Theoretical studies are now able to describe semi-quantitatively epitaxially induced alloy stabilization[18-20] as well as the dynamics of non-isovalent metastable growth.[21] However, the list of thermodynamically-immiscible semiconductor components is far longer than the few examples cited above, so there is an urgent need to survey them theoretically, predict their phase-diagrams and growth kinetics, and attempt off-equilibrium growth of the most promising candidates.

To summarize, the basic research opportunities in this area are

- theory and measurements of bowing parameters of non-isovalent pseudo-binary systems such as II-VI/IV-IV, III-V/IV-IV, and II-VI/III-V,
- theory and measurements of bowing of non-isostructural alloys such as chalcopyrite/zincblende,
- theory of phase-stability of thermodynamically forbidden alloys, and
- off-equilibrium growth of thermodynamically insoluble components.

These areas of research are likely to considerably broaden the material base available to electronic devices without using superlattices or other complex quantum structures.

USE OF REDUCED DIMENSIONALITY STRUCTURES FOR PHOTOVOLTAIC DEVICES

In this section, we propose the use of reduced dimensionality namely 2D, 1D, and 0D carrier confining structures as a powerful approach to novel photovoltaic structures. The main arguments in favor of the reduced dimensionality structures are:

- The stronger absorption compared to bulk semiconductors: The increased density of states that comes with a reduction of the dimensionality leads to a much stronger absorption as the structure goes from 3D to 2D, 1D, and 0D. This is an overwhelming advantage over the double heterostructures especially for very thin superlattices since the photovoltaic device characteristics are optimized for very thin films.
- An enormous flexibility in device design that comes with the band gap engineering that is possible with 2D, 1D, and 0D superlattices. This has been exploited in the past ten years through the demonstration and production of a multitude of semiconductor devices based on quantum wells and superlattices.[22]
- The possibility of separating the absorber and carrier collection regions. This advantage has already been demonstrated in the superlattice n-

i-p-i photodiode structures[23] that permit a separation of electrons and holes in direct space.
- By using band gap engineering and extracting carriers in a direction parallel to the interface, such lateral superlattice structures could become superior to the double heterostructures. Indeed, in Group III-V compound semiconductors for example, the short minority carrier lifetimes that are due to alloy scattering (in ternary and quaternary alloys) can be compensated by extracting the carriers into the small band gap (binary) regions of the superlattice.

Here again, research on the physics of the devices and modeling should be undertaken before work on the device manufacturing is started. However, over the past ten years a huge body of information on band gap engineering of superlattices and low dimensional device structures has been accumulated in the literature and extensive use of this data base could be made for PV applications. We start, therefore, by describing the basic design principles of band gaps through a superlattice-type layering of two materials. The plan of this section is to discuss (a) tuning band gaps by using superlattice quantum-confinement without strain, (b) using strain to tune band gaps in strained layer superlattices, (c) using lateral superlattices, (d) using free-standing nanocrystals, (e) using zeolite-confined nanocrystals, and (f) using one-dimensional organic semiconductors.

Band Gap Tuning Through Superlattice Quantum Confinement Without Strain

Suppose that one is given two semiconductors and asked to form a material with an intermediate band gap without mixing them. The basic idea here is to take the semiconductor with the small gap (SG) and layer it in a $(SG)_p/(LG)_q$ superlattice geometry with a lattice-matched material having a larger gap (LG). For small layer thicknesses (p,q), quantum confinement acts to lower the valence-band maximum (VBM) and raise the conduction-band minimum (CBM), thus increasing the superlattice gap above that of pure SG. This was proposed theoretically by Tsu and Esaki.[24a] More recently this was also suggested for SG = HgTe and LG = CdTe by Schulman and McGill[24b] and by Smith et al.[25] and examined experimentally by Reno and Faurie.[26] The same principle has been used to engineer various band gaps in the AlAs/GaAs system. There are two less-recognized aspects to this widely-used method:
- use of orientation-dependence for tuning band gaps, and
- considering the effect of superlattice interdiffusion on band gaps.

These are briefly discussed below.

Use of Orientation to Tune Band Gaps of Short-Period Superlattices

Much of the research on semiconductor superlattices uses a fixed growth orientation; e.g. (001) for Group III-V systems. There are, however, intriguing opportunities of changing the optical properties by selecting different orientations. While long (strain-free) superlattices $(AC)_p(BC)_q$ and $(p,q)\rightarrow\infty$ have the same band gaps for all AC/BC layer orientations, short-period superlattices have band gaps that depend on the layer orientation. This provides an interesting degree of freedom for superlattice band gap engineering without strain. The theory for this was outlined in Ref. 27, and is based on the different folding relationships for different superlattice (SL) orientations. For example, Ref. 27 predicted that (111)-oriented AlAs/GaAs SLs will have direct band gaps despite the fact that short-period AlAs/GaAs SLs oriented along (001) are known to have an indirect band gap. Recent experimental results[28] have failed, however, to find a direct gap in (111)-oriented AlAs/GaAs SLs. The authors[27] believe, however, that these (111) samples may not exhibit sufficiently abrupt interfaces to reveal the properties of true (111) SLs (measurement of piezoelectric effect could be instrumental here). This effect is discussed next, as it offers an additional opportunity of band gap engineering through control of interfacial roughness.

Effect of Interfacial Nonabruptness on Band Gaps

As mentioned above, currently grown superlattices may not exhibit atomically abrupt interfaces even in strain-free systems such as GaAs/AlAs. Gell et al.[29] and Laks and Zunger[30] have recently formulated theoretical approaches that predict the value of the band gap as a function of the interfacial roughness. It was shown, for example,[30] that while in an abrupt (001)-oriented monolayer GaAs/AlAs superlattice, the lowest gap (1.93 eV) is an L-derived GaAs-like state, in a locally interdiffused SL the gap reverts to the 2.08 eV X^{xy}-derived AlAs state. This suggests the possible use of the degree of interfacial abruptness as a new degree of freedom in tuning band gaps.

To summarize, the main research opportunities in this area are experimental and theoretical design of orientation-dependent band gap tuning, and control of the SL band gaps through control of SL interfacial abruptness. These rather unexplored degrees of freedom could be used in conjunction with the rather mature field of lattice-matched superlattice growth, thus diversifying the materials properties.

Superlattice Strain-Induced Band Gap Tuning

Biaxial strain can be used to reduce band gaps. The basic idea here is to take a material with a small band gap and small lattice constant (SGSL) and layer it coherently with a material having a larger gap and larger lattice constant (LGLL), forming a strained-layer $(SGSL)_p/(LGLL)_q$ superlattice. Coherence of SGSL with LGLL then expands the lattice constant of SGSL parallel to the interface, thus lowering its Γ conduction-band minimum. At the same time, tetragonal compression of SGSL in the perpendicular direction splits its valence band maximum, raising the energy of the upper split components. Both effects

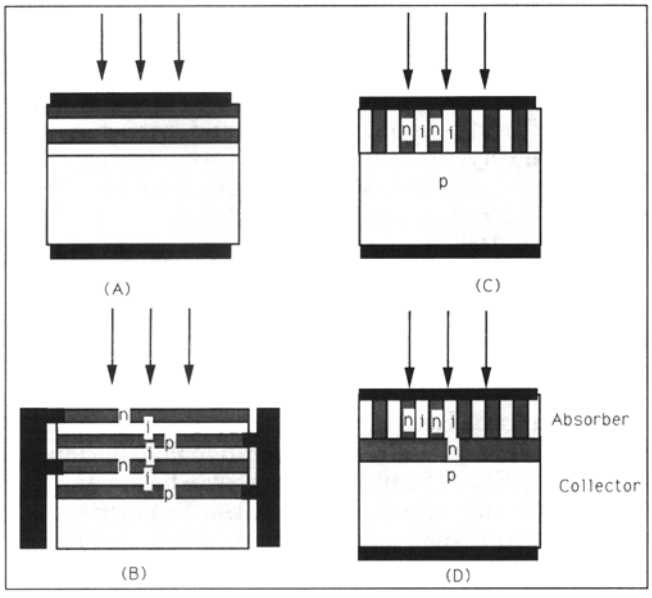

Fig. 1. (a) Cross-sectional view of a conventional superlattice with the photocurrent collection perpendicular to the interfaces. (b) An n-i-p-i structure superlattice with a lateral current collection. (c) A possible lateral superlattice structure with current collection perpendicular to the interface. (d) A possible lateral superlattice structure with a separate absorber and collector section. In all these schematics, the contacts are indicated by solid areas and the wide and small band gap regions in the device are shown as shaded and unshaded areas respectively.

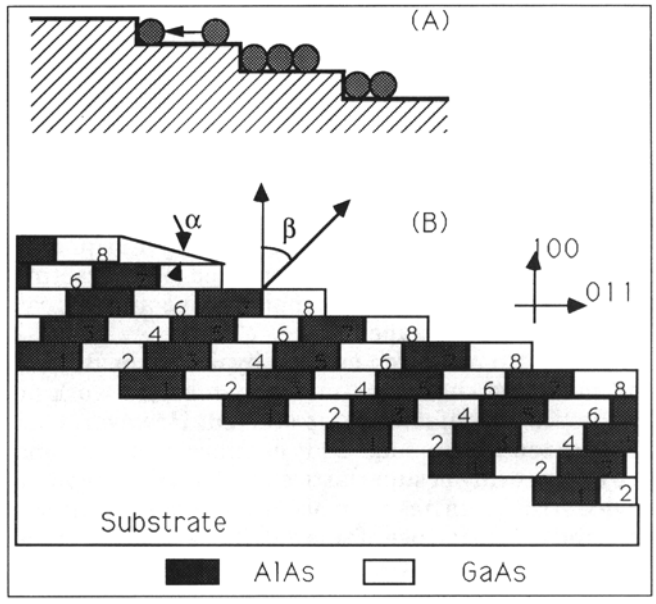

Fig. 2. (a) Schematic of the step flow growth regime required for the lateral superlattice (LSL) growth. (b) Schematic of the deposition sequence for a tilted LSL. The numbers indicate the deposition sequence for the fractional monolayers.

act to reduce the band gap relative to unstrained bulk SGSL. This approach has been proposed by Osbourn[31] for SGSL = $InAs_{0.39}Sb_{0.62}$ and LGLL = $InAs_{1-x}Sb_x$ with x>0.61. Since quantum confinement effects at small (p,q) act in the opposite direction (increasing the band gap) relatively thick layers are needed to achieve the maximum band-gap narrowing.[31,32] Yet, the need to accommodate coherently the misfit strain limits the maximum thickness that can be used.

Biaxial strain has also been used recently to make a few predictions

- use of strain to convert the normally-indirect $(GaAs)_1(GaP)_1$ SL grown on a lattice matched substrate into a direct gap superlattice $(GaAs)_1(GaP)_1$ grown on GaAs[33] (rather than growing it on the lattice-matched alloy). There are now experimental confirmations of this idea.[34]
- use of strain to convert the indirect gap Si_nGe_n SL grown on Si to a direct gap SL when grown on $Si_{0.5}Ge_{0.5}$ or on pure Ge substrates.[35] The experimental results here are yet inconclusive; there are, however, strong ongoing interactions between experimentalists and theorists to clarify this situation.[36]

Again, the research opportunities here are almost unlimited, once one realizes the basic design principle of use of biaxial strain.

Direct Growth of Lateral Superlattices for Photovoltaic Structures

The difficulty in collecting and transporting carriers efficiently in conventional superlattice structures (or, for that matter, in double heterostructures) has been in our opinion, one of the main barriers to their application to photovoltaic structures. This problem is definitely not as severe if one uses lateral superlattices. This idea is schematically illustrated in Fig. 1. The lateral superlattice structure also offers greater flexibility in designing within the structure a separate absorber and collector region.

There are at least two approaches to the growth of lateral superlattices (LSL): sequential deposition of submonolayers of materials A and B on a misoriented, stepped substrate,[37–39] and use of spontaneous lateral phase separation perpendicular to the growth direction of short-period superlattices.[40]

In the first method, the orientation of the quantum well with respect to the substrate surface, as well as their thickness, are continuously changed during growth. The basic principle for this epitaxial growth method was developed and demonstrated several years ago.[37,38] It involves the alternate deposition of fractional submonolayers m and n (m, n <1) of two semiconductors $(A)_m(B)_n$ with different band gaps on a substrate comprising a well-ordered array of steps. The ordered vicinal surface is made of mono-atomic steps with a periodic spacing LxL may be adjusted by choosing the substrate vicinal angle and the ordering of the steps by growth of a buffer layer in the step flow growth regime. This LSL growth method has been successfully demonstrated both by molecular beam epitaxy[37] (MBE) and metal organic chemical vapor deposition[39] (MOCVD) for the GaAs-AlGaAs system. It has also been applied successfully to the GaSb-AlSb system[41,42] and, with the appropriate growth conditions, should be applicable to a wide variety of semiconductors or even metal or insulators systems. This growth method has successfully been used to demon-

strate 2D quantum confinement by optical methods.[42-43] Its attractiveness stems from its simplicity for producing lateral superlattices with variable shapes, periods and, therefore, band gaps. The deposition method is schematically shown in Fig. 2. The tilt angle β as well as the superlattice or quantum well period is continuously adjustable by tuning the layer coverage parameter p = m + n. The lateral superlattice can be conveniently shaped to produce an additional degree of carrier confinement in the structure. Indeed, a linear variation of p between two values $p_A<1$ and $p_B>1$, as a function of layer thickness leads to the formation of quantum wells with parabolic interfaces. The meandering interfaces of the quantum wells as well as their thickness is varying along the substrate normal direction. The superlattices formed (Fig. 3) are called serpentine superlattices.[43] One coverage cycle corresponds to the deposition of m monolayer of $(AlAs)_m$ or $(AlGaAs)_m$ followed by n monolayer of $(GaAs)_n$ with m and n<1. If the cycle coverage is repeated and kept constant during the growth, a transverse superlattice is obtained. The curvature K of the parabola is directly related to the quantum confinement along the growth direction while the lateral confinement is determined by L, the step period. This curvature may be chosen at will since it is determined by the linear ramping rate of the per cycle coverage with

$$K = 2[P_B-1]/\tan(\alpha) \qquad (2)$$

where α is the substrate misorientation angle. The proposed photovoltaic material would contain a series of parabolic or serpentine superlattices with variable curvatures. The effective band gap of these parabolic wells would be adjusted by the curvature. This structure is expected to show a broad absorption spectrum that is essentially limited by the band gap of the quantum well material at the low energy end of the spectrum.

A second method of growth of lateral superlattices has recently been demonstrated by Hsieh et al.[40] In this method, one grows a (001) oriented short-period A_n/B_n superlattice (n~2) on a flat substrate, adjusting the fluxes of A and B so that they are slightly off-stoichiometry; i.e. $A_{n+\varepsilon}B_{n+\varepsilon'}$. If the materials A and B are size-mismatched (e.g. A=GaP; B=InP), one finds in the plane perpendicular to the growth direction a periodic array of composition-modulated lateral superlattices; e.g. a ~200 Å period $(Ga_xIn_{1-x}P)/(Ga_yIn_{1-y}P)$ superlattice with x ~0.45 and y ~0.55. Quantum-confinement in the lateral direction has been observed spectroscopically.[44]

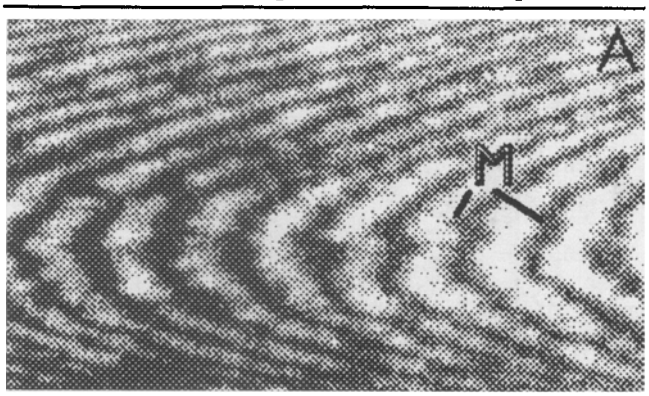

Fig. 3. Cross-section transmission electron diffraction (TED) and micrographs (TEM) of GaAs-AlGaAs serpentine superlattice containing array of quantum wires. The vicinal substrate orientation is two degrees. The white and dark areas correspond, respectively, to the barrier (Al rich regions) and quantum well (Al poor regions).

These lateral superlattice structures should exhibit excellent photo carrier collection efficiency because of the high quality quantum well interfaces. Doping of these structures has been demonstrated, and the carrier collection should be efficient because the carrier transport occurs parallel to the interfaces.

Nanocrystalline and Two-Phase Semiconductors

Nanocrystalline semiconductors are intriguing materials. Their optical properties are affected by light scattering and by carrier confinement, and the carrier scattering lengths are of the order of crystallite size. Nanocrystalline silicon[45] is a two-phase material, with cluster-like silicon crystallites embedded in a hydrogen-rich matrix. The strong subgap optical absorption of nanocrystalline silicon suggests a high density of gap states. The minority carrier collection properties suggest a high density of gap states or carrier confinement by the hydrogen-rich mantle around the silicon clusters. Because the cluster size is comparable to the electron wave function, the scattering and the diffusion length, nanocrystalline semiconductors are quite complex materials, which offer themselves as vehicles for highly tailored optoelectronic properties. Two-phase materials with larger grains also might exhibit desirable combinations of optical absorption and carrier transport. The introduction of nanocrystalline semiconductors to photovoltaics requires learning the controlled and reproducible growth of nanocrystalline dispersions. The opto-electronic properties must be studied in function of the structure of these dispersions, and the materials must be introduced to experimental photovoltaic devices.

Nanocrystalline Materials in Zeolite Cages

A novel and potentially important technology for the fabrication of structures with two or three degrees of carrier confinement is based on filling of natural (or synthesized) three-dimensional cage crystalline or amorphous templates that are then used for the epitaxy of semiconductors. The zeolite materials are candidates for this approach since the cage dimensions are in the nanometer scale.[46a]

Formation of Mesoporous Zeolite Structures

For the processing of the nanocrystalline structures, we propose to load a zeolite matrix with a

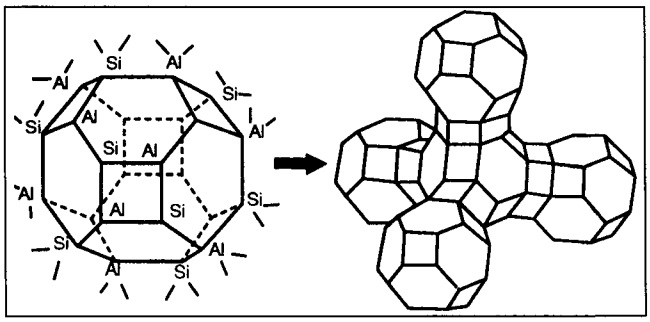

Fig. 4. Schematic of the cage structure of a Y zeolite.

semiconductor. The zeolite consists of a wide band gap silica-aluminate or SiO_2. These mesoporous zeolite structures are synthesized from a lipid micelles solution doped with Si.[46a] After annealing of this solution, a powder consisting of polycrystalline zeolite is obtained. Transmission electron microscopy (TEM) indicates micron size grains comprising an array of mesoscopic tubes. High resolution TEM further indicates that the tubes form a regular hexagonal array. The mesoscopic tube diameter can be adjusted from 20 Å to 100 Å by using the proper micelle solution chemistry. The tube length is adjusted by the grain size (0.1–1 μm) that is controlled by the growth conditions. Transmission electron diffraction (TED) and x-ray diffraction show only diffraction peaks that are associated with the hexagonal tube array. The absence of additional diffraction peaks suggests that the SiO_2 molecules in the tube walls are not arranged in a crystalline lattice with long range order. The next step is to attempt loading such structures with semiconductors and test their absorption and transport properties.

Formation of Nanoscopic Zeolite Structures

The microscopic zeolite structures can also be formed by wet chemistry and dehydration. A solution comprising cations (K^+ or Na^+) or micelles and silica aluminates is used for the synthesis of the zeolite. The structure is self-assembling. The hydroxyl molecules are removed from the structure by annealing. Transmission electron microscopy, x-ray, and neutron scattering experiments indicate that the silica aluminate zeolite structures contain a periodic array of cages with a diameter of 13 Å. Fig. 4 gives a rendering of the cage assembly for the dehydrated zeolites that forms a three-dimensional network with a very large unit cell (25 Å lattice parameter). The cages are connected to each other by 12-sided faceted tubes that have a diameter of 9 Å forming a tetrahedral assembly of supercages. Transmission electron microscopy analysis indicates that the zeolite cages are assembled into polycrystalline powder with micron size grains.

Loading of the Zeolite Cages

A method that permits epitaxy of the semiconductor inside the zeolite cages is desirable. We propose to use a vapor phase technique that permits a succession of loading, cracking, and annealing cycles. One of the nontrivial problems to solve is that of the vapor diffusion inside the tubes without plugging them by the deposited semiconductor. Hence, it is essential to separate the loading (diffusion) cycle from the cracking cycle that is taking place at a higher temperature. A repeated sequence of loading and cracking cycles was found to be a convenient way of loading the zeolite structures. The semiconductor epitaxy is then completed by an annealing cycle. The entire process is monitored with a quadrupole mass spectrometer. Weight change measurements upon loading of the zeolite permit an assessment of the zeolite loading.

Tomiya et al.[46b] have performed such experiments using a Y zeolite cage matrix and germanium as the prototype semiconductor. Germane vapor was loaded in the zeolite cages. The presence of germanium was ascertained from the quadrupole mass spectrometer that showed the large germane incorporation and only release of hydrogen during the cracking cycle. Transmission electron microscopy, TED, and x-ray diffraction do not indicate the presence of germanium crystalline lines in these loaded zeolites. X-ray diffraction lines exhibit intensity changes and a small (0.2%) lattice expansion. X-ray energy dispersive analysis with the scanning TEM shows strong germanium lines, indicating that at least 10^{20} germanium atoms/cm^3 are present in the zeolite structure. It is presently believed that the germanium is present in a crystalline form that is commensurate with the zeolite lattice. These powder samples exhibit a strong luminescence band centered around 7500 Å (Fig. 5). The origin of this luminescence is presently analyzed by performing absorption and excitation luminescence measurements.

The size uniformity issue in these nanocrystals is related to the loading uniformity of the supercages as a function of their distance from the zeolite grain surface. We believe that using this loading method, both the zeolite and mesoscopic zeolite structures can be loaded with semiconductors. The example given here with germanium could easily be duplicated with silicon and other semiconductor materials such as

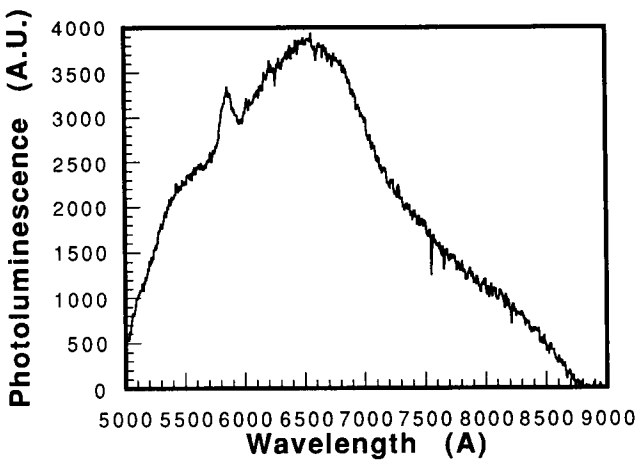

Fig. 5. Room temperature photoluminescence spectrum of a germanium Y zeolite loaded structure.

GaP or GaAs or ZnSe.

The graphoepitaxial process could in fact play an important role in the formation of the semiconductor nanocrystals especially in the case of the mesoscopic zeolite structures which have amorphous walls. In proposing this approach for photovoltaic cells, we are of course hoping to reach the very high absorption coefficient expected from the 0D semiconductor network formed in this manner. The close proximity of the nanocrystals could ensure that a tunneling process will provide a transport process for the photocarriers. Doping of these structures is hopefully readily achievable. Transport would take place by tunneling of carriers from one cage to another.

Organic Semiconductors

Organic dye molecules can be made very strong optical absorbers,[47] and they promise manufacturability in foils and films. When used for solar cells[48] that are analogous to conventional photodiodes, organic semiconductors have suffered from two disadvantages. One is that the conventional deposition techniques introduce disorder which causes excessive carrier trapping. Recently, the preparation of single-crystalline organic films for optoelectronic applications has been demonstrated;[49] it could be extended to solar cells. The second, and more fundamental, difficulty with organic absorbers is that they are built up of isolated, instead of connected, molecules—photogenerated excitations, including charge carriers, must cross over from one molecule to the next to extract their energy. During tunneling and the associated trapping, much energy is lost. Therefore, we should seek to develop cross-linked organic systems in which the highly conducting π-electronic system of the light-absorbing chromophores is left intact. This work likely will rely on a collaboration between dye and metalorganic chemists and semiconductor physicists.

BAND GAP REDUCTION THROUGH SPONTANEOUS ORDERING OF SEMICONDUCTOR ALLOYS

It has recently been noted that numerous Group III-V alloys exhibit in vapor phase growth spontaneous long-range ordering in the form of monolayer $(AC)_1/(BC)_1$ superlattices in the (111) orientation (the CuPt-like structure). The degree of ordering is never perfect; it can however, be maximized in certain growth temperature ranges and substrate misorientations. An extended list of observations of CuPt ordering is given in Ref. 19. In all cases, ordering occurred as a result of homogeneous alloy growth without sequential (shutter-controlled) exposures. Refs. 50 and 51 provide a general survey of some of the main observations.

It is now understood that surface reconstruction could be responsible for the CuPt type spontaneous ordering in size-mismatched alloy. Figure 6 shows, for example, the calculated order parameter for a cation-terminated (001) $Ga_{0.5}In_{0.5}P$ surface as a function of temperature.[52] We see that if reconstruction is

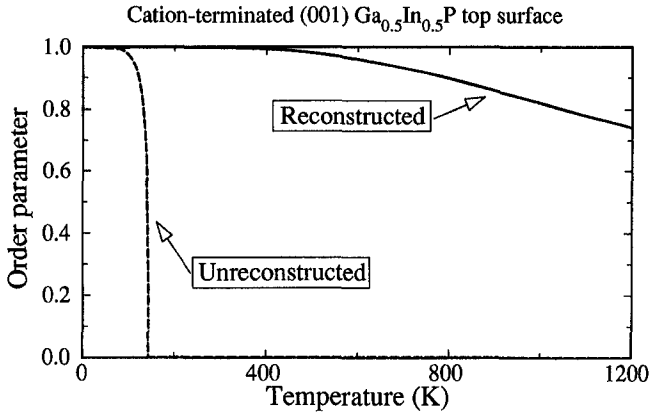

Fig. 6. Calculated[51] order parameter η for a (001) cation surface of $Ga_{0.5}In_{0.5}P$ as a function of temperature. When the surface is unreconstructed (dashed line) the fully ordered (η = 1) structure disorders into the random alloy (η = 0) at very low temperatures. When surface reconstruction is included (solid line), significant ordering persists at growth temperatures (~1000 K).

neglected (dashed line) the CuPt ordering (η = 1) disappears at very low temperatures, so at growth temperatures one expects but a random alloy (η = 0). On the other hand, if surface reconstruction is included in the calculation (solid line), significant ordering persists even at growth temperatures. This shows that surface thermodynamics play a crucial role in promoting ordering. Naturally, growth kinetics would determine the extent of ordering, hence manipulation of growth parameters (choice of precursors, growth rates, fluxes, etc.) could maximize the size of the ordered alloy and the degree of ordering.

This unique phenomenon of spontaneous ordering was predicted to alter the alloy's band gap in a significant way.[51] The basic reason can be appreciated as follows. Denoting superlattice (SL) states by an overbar and the homogeneous alloy states by angular brackets, folding relations show that in a monolayer $(AC)_1(BC)_1$ (111) superlattice the states at the $\bar{\Gamma}$ point are constructed from zincblende-like states at $\langle\Gamma\rangle + \langle L^{111}\rangle$. The folded zincblende states at this wave vector are coupled by the perturbing superlattice potential $\delta V(\mathbf{r})$. This coupling leads to a level repulsion between states of the same symmetry; i.e. the superlattice states are displaced relative to the unperturbed states. For example, the $\bar{\Gamma}$-folding alloy states $\langle\Gamma_{1c}\rangle$ and $\langle L_{1c}\rangle$ couple through δV, producing the superlattice states $\bar{\Gamma}_{1c}^{(1)}$ and $\bar{\Gamma}_{1c}^{(2)}$ that are lowered and raised, respectively relative to the averages alloy states. The downward displacement of the $\bar{\Gamma}_{1c}^{(1)}$ (the conduction band minimum, or CBM) and the upward displacement of the $\bar{\Gamma}_{3v}^{(2)}$ (the valence ban maximum, or VBM) reduce the band gap. Theoretical details describing this mechanism are given in Ref. 51. Fig. 7 shows predictions for band gap reductions through spontaneous ordering for many systems. It illustrates how the direct band gap of the random alloy at $x = \frac{1}{2}$ changes if the alloy orders in the monolayer (201) structure (chalcopyrite) the (001) structure (CuAu), or the (111) structure (CuPt).

This mechanism can lead to the interesting op-

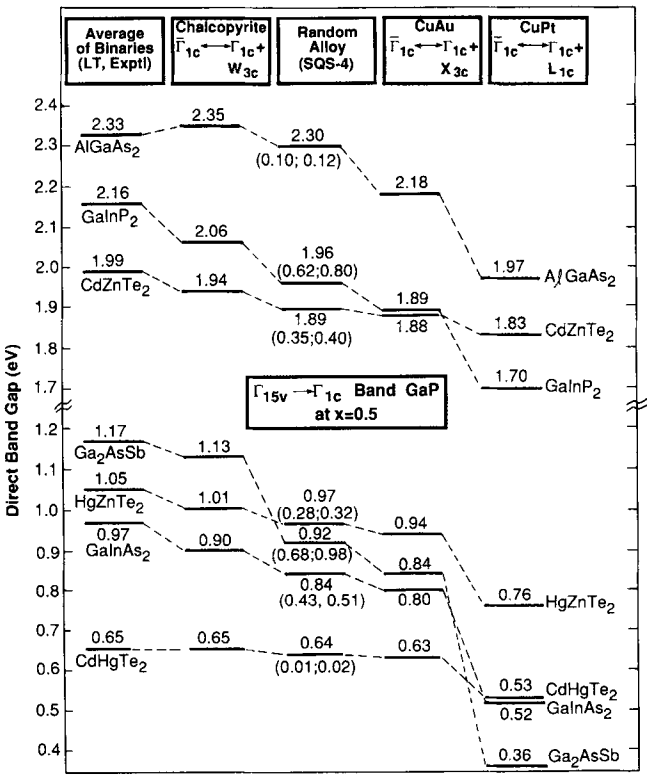

Fig. 7. Predicted direct band gaps at composition x = 1/2 for random alloys and various ordered alloys [Wei and Zunger, *Appl. Phys. Lett.*, 56 (1990), p. 662]. Results are shown for (201), (001), and (111) orderings, termed, respectively, chalcopyrite, CuAu, and CuPt.

portunity of tuning alloy band gaps at a fixed composition, by selecting those growth conditions that induce spontaneous ordering. Ref. 51 lists many common semiconductor alloys and gives their predicted band gaps for a few forms of crystallographic order. Such effects have also been seen experimentally.[53] This mechanism or ordering-induced band gap narrowing has been recently proposed[54] to yield ~10 μ band gap in spontaneously-ordered $Ga_{1-x}In_xSb$ and $InAs_{1-xe}Sb_x$ alloys. Initial experimental results[55] appear very encouraging.

It was pointed out[54] that the band gap reduction depends (quadratically) on the degree η of long range ordering. Hence, a variable gap over a significant spectral range can be obtained by controlling the degree of ordering. There are clearly many research opportunities here in growing and characterizing the optical properties of such novel ordered alloys (see Fig. 7).

BAND GAP MANIPULATIONS THROUGH DIRECT CHEMICAL SYNTHESIS

In the previous sections, we have discussed the basic principles of band gap engineering through *physical* means of alloying, or the application of weak external fields such as strain or geometric confinement. Of course, the traditional way that chemists use to change the properties of materials is through chemical means; i.e. direct synthesis of new species. The possibilities here are almost endless. For instance, the compilation of Landolt and Bornstein[3] lists a few hundred nontraditional semiconductors whose properties are largely unexplored, but whose band gap values are potentially attractive to a number of opto-electronic applications. To keep our discourse reasonably concise, we will limit ourselves here to simple semiconductor structures that can be derived from the zincblende structure by atomic transmutations. We have in mind three classes of semiconductors:

- *Interstitial compounds.* These can be derived from the AC zincblende structure by splitting the A atom into two elements A′ and A″ whose combined valence equals that of A. One of the two elements (say, A′) will reside on the zincblende site (occupied previously by A), while A″ will occupy one of the tetrahedral interstitial sites, that is empty in the zincblende structure. Simple examples of such compounds include the known $A_2^{II}Si$ antifluorite family[56] (e.g. Mg_2Si) obtained by splitting Si → Mg + Mg, and the Nowotny-Juza family $A^IB^{II}C^V$ (e.g. LiZnP) obtained by splitting Ga in GaP to Ga → Li + Zn. Table II lists the known compounds belonging to this family.

Table II. Known Nontransition Metal $A^IB^{II}C^V$ Filled Tetrahedral Semiconductors

Compound	a(Å)	Known Property	Ref.
LiBeP	10.24 = a 12.03 = c		a
LiMgN	4.970	red-brown	b
LiMgP	6.023	brown	c
LiMgAs	6.21, 6.05		d,e
LiMgSb	6.62		d
LiMgBi	6.75		d
LiZnN	4.877	black	b
LiZnP	5.76	brown	c
LiZnAs	5.924	black	b
LiZnSb	—		
LiZnBi	—		
LiCdP	6.087	black*	f
NaZnAs	5.912		g
NaMgAs	a = 4.42, c = 7.05		h
KZnAs	—		
CuMgP	—		
CuMgAs	a = 3.961, c = 6.238		i
CuMgSb	6.152		i
CuMgBi	6.256		i
CuZnAs	5.872		j
CuCdSb	6.262		b
AgMgP	—		
AgMgAs	6.240		i
AgMgSb	—		
AgZnAs	5.912		g

* Alloys with LiZnP.

Note: In most cases, only the lattice parameters and color were established. See Ref. 57 for calculated properties of some members.

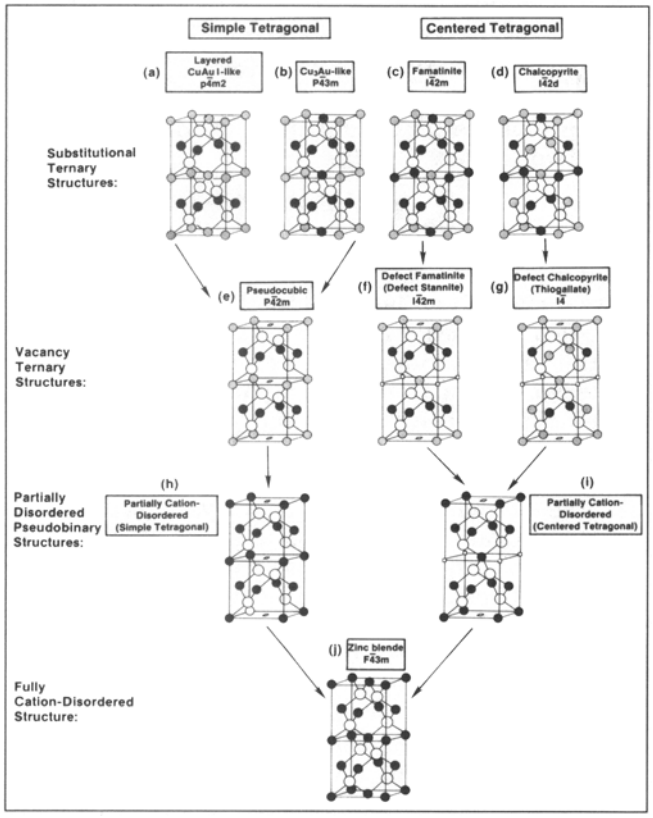

Fig. 8. Various types of ordered vacancy structures that can be obtained from simple semiconductors. See Ref. 64.

- *Substitutional compounds.* These can be obtained conceptually by taking two formula units of a Group III-V compound (e.g. $2GaP = Ga_2P_2$) and shifting a proton from one cation to the other: $^{31}Ga + {}^{31}Ga \rightarrow {}^{30}Zn + {}^{32}Ge$. This gives $ZnGeP_2$, or more generally, $A^{II}B^{IV}C_2^{V}$. Similarly, carrying out the same process for $2ZnS = Zn_2S_2$ gives $^{30}Zn + {}^{30}Zn \rightarrow {}^{29}Cu + {}^{31}Ga$, or $CuGaS_2$. More generally, this yields the $A^{I}B^{III}C_2^{VI}$ chalcopyrite family.
- *Ordered vacancy compounds.* These are derived from the parent zincblende compound by fusing two cations into a single cation with doubled valence, leaving one sublattice vacant. A simple example is to take two formula units of $2CuInSe_2 = Cu_2In_2Se_4$, then fuse $2Cu \rightarrow Cd$, creating $CdIn_2Se_4$ with an ordered array of vacancies. Fig. 8 shows how many families of semiconductors can be constructed in this way.

What follows is a brief account of the current theoretical status in these areas and what is known experimentally. We will further discuss as a separate class the possible use of compounds with d or f electrons.

Interstitial Semiconductors Based on the Zincblende Structure

This group includes the Nowotny-Juza filled tetrahedral semiconductors $A^{I}B^{II}C^{V}$. Table II lists those that were synthesized early on. Other than the crystal structure and the color, nothing was known about these materials. The electronic structure of many of these materials was recently calculated.[57] It was found that even when the parent zincblende compounds (e.g. GaP, GaN) have indirect band gaps, the corresponding filled structures (e.g. LiZnP or LiZnN) have direct band gaps. Following this work, some of these materials were recently synthesized and characterized.[58] This family clearly includes a large number of structurally simple semiconductors with a wide range of band gaps. Most of these are unexplored.

Substitutional Semiconductors Based on the Zincblende Structure

This group includes the ternary chalcopyrites $A^{I}B^{III}C_2^{VI}$ and pnictides $A^{II}B^{IV}C_2^{V}$; many of them are well known.[59] However, one can easily make a list of chalcopyrites and pnictides that so far have not been made. Martins and Zunger[60] and Jaffe and Zunger[61] have calculated the band structures of a number of yet unmade chalcopyrites. Jaffe and Zunger[62] have predicted the band gaps and lattice structure of 22 yet-unsynthesized chalcopyrites and pnictides. This was done by starting from the band gaps of the parent binary zincblende structure and calculating the change in band gaps due to p-d coupling present in the ternary, and bond relaxation ($R_{AC} \neq R_{BC}$ in ABC_2). Results are given in Table III. As can be seen, these provide a range of potentially useful band gap values. To our knowledge, none of these materials have been made.

Ordered Vacancy Compounds

Fig. 8 shows the type of semiconductor structures that can be constructed by introducing an ordered array of vacancies. Parthé[63] lists a large number of these compounds. Experimental data on the $A^{II}B_2^{IV}C_4^{VI}$ is summarized in Ref. 64 that also describes the calculated electronic structure of this family. Clearly, ordered vacancy compounds provide a rich menu of yet unexplored zincblende-like semiconductors.

Compounds with d or f Electrons

Much of the research on new photovoltaic semiconductors has focused on materials with diamond-like structures, whose valence and conduction bands are made up largely of s and p electrons. A very large number of semiconductors incorporating transition elements and exhibiting other crystal structures does exist and may be interesting for photovoltaic application.[65] Examples are Cu_2S, Zn_3P_2, WSe_2, and FeS_2. Such semiconductors could be valuable because of very strong optical absorption, or because they are composed of inexpensive constituents. No useful guidelines exist for the identification of such semiconductors, so that empirical synthesis and evaluation, as well as theoretical tools for their identification are desired.

BIOMIMETIC STRUCTURES

In classical photovoltaic devices, both the charge separation in energy (producing voltage) and the

Table III. Predicted[62] Structural Parameters and Estimated Band Gaps for 22 Possible Chalcopyrite-Structure Semiconductors

Compound	a (Å)	u	η	E_g (eV)
$ZnSiSb_2$	6.077	0.270	0.961	0.9
$ZnGeSb_2$	6.111	0.263	0.975	0.5
$CdSiSb_2$	6.344	0.291	0.921	0.8
$CdGeSb_2$	6.383	0.285	0.933	0.2
$MgGeP_2$	5.656	0.277	0.947	2.1*
$MgSnP_2$	5.774	0.250	1.000	1.8
$MgSiAs_2$	5.804	0.284	0.935	2.0*
$MgGeAs_2$	5.841	0.276	0.949	1.6
$MgSnAs_2$	5.958	0.250	1.000	1.2
$MgSiSb_2$	6.221	0.281	0.939	1.4
$MgSiSb_2$	6.258	0.275	0.952	0.9
$MgSnSb_2$	6.374	0.250	1.000	0.6
$HgSiP_2$	5.740	0.296	0.913	1.6
$HgGeP_2$	5.780	0.288	0.927	1.2
$HgSnP_2$	5.909	0.262	0.977	0.8
$HgSiAs_2$	5.926	0.294	0.916	0.7
$HgGeAs_2$	5.966	0.287	0.929	0.2
$CuTlTe_2$	6.299	0.233	1.034	0.9
$AgTlS_2$	5.882	0.257	0.986	1.1
$AgTlSe_2$	6.113	0.257	0.986	0.7
$AgTlTe_2$	6.529	0.257	0.987	0.6
$BeCN_2$	3.847	0.313	0.883	8.2*

*Indicates compounds most likely to have a pseudodirect gap; a is the lattice constant, u is the dimensionless cell-internal structural parameter, $\eta = c/2a$ is the tetragonal ratio.

charge separation in space (producing current) is done with electrons and holes. Biological photoconverters employ many combinations of electronic excitation with electronic and ionic charge separation.[66,67] For example, the energy provided by the electronic excitation may be channeled into a change in conformation of the protein which carries the light-absorbing chromophore. The consequence of this change in conformation is ionic charge transport, usually via the severing and formation of hydrogen bonds, a process whose net effect is hydrogen ion motion.[68] In this way, the optical excitation drives a hydrogen ion pump, providing the energy for the synthesis of ATP from ADP. A fundamental study of charge separation by ionic transport in synthetic analogs of such biological systems may lead to the identification of nonelectronic alternatives for charge transport, or of charge transport directly combined with energy storage.

STRUCTURES WITH SEPARATED ABSORBER AND TRANSPORT MATERIALS

Spatial separation of the functions of electronic excitation from charge transport may allow optimizing the two functions separately, opening the prospect of obtaining higher efficiency. The structures best suited to this function will combine islands of the absorber embedded in a matrix of a smaller-gap transport material. Such structures could be made by random nucleation of growth of a second phase in a starting material, or by controlled alternating growth of the two phases.

SUMMARY

This paper outlines the general principles that afford controlled design of semiconductor band gaps. These involve four classes of methods:

- Use of physical mixing (i.e. alloying). The essential research opportunities here involve characterization of the bowing phenomena in unexplored non-isovalent (Group II-VI/IV; II-VI/III-V, and II-VI/IV) and in non-isostructural (e.g. chalcopyrite/zincblende) systems (Table I).
- Use of reduced dimensionality. This includes tuning gaps by formation of superlattices without and with strain, the use of lateral superlattice geometries, the use of free-standing as well as cage-confined nanostructures, and the use of one-dimensional organic semiconductors.
- Use of spontaneous ordering of semiconductor alloys to obtain new materials.
- Use of direct chemical synthesis. This includes among others, new interstitial compounds derived from zincblende (Table II), new substitutional compounds derived from zincblende (Table III), ordered vacancy compounds (Fig. 8), and compounds with d or f electrons.

These principles of photovoltaic architecture constitute just a few simple examples, aimed at illustrating how structural chemistry and solid state theory can be used to significantly increase the data base of technologically useful semiconductors. Clearly, collaborative efforts among the new material predictor, material grower, and material characterizer, could potentially lead to the systematic discovery of new and exciting semiconductor materials.

ACKNOWLEDGMENTS

A. Zunger's work on this paper was supported by the Office of Conservation and Renewables and by the Office of Energy Research, Basic Energy Sciences, Division of Materials Science, U.S. Department of Energy. P. Petroff wishes to thank G. Stucky, V. Srdanov, and S. Tomiya for making available their results on the zeolite structures. Part of the work of P. Petroff was supported by grants from the AFOSR (# 88-0334) and QUEST and the National Science Foundation Science and Technology Center (Grant DMR 88-10430). S. Wagner wrote part of this paper while a visiting scientist at the Electrical Power Research Institute (EPRI) in Palo Alto, California. He wishes to thank EPRI's storage and renewable department and EPRI's Office of Exploration and Applied Research for their invitation, and Dr. Terry M. Peterson for valuable discussions and for his hospitality.

REFERENCES

1. Recent books summarizing modern electronic structure methods include *Electronic, Structure, Dynamics, and Quantum Structural Properties of Condensed Matter,* eds. J.T. Devereese and D. Van-Camp (New York: Plenum, 1985). Also, *The Electronic Structure of Complex Systems,* Vol. 113 of NATO Advanced Study Institute, eds. P. Phariseau and W.M. Temmorman (New York: Plenum, 1982).
2. J.C. Woolley, *Compound Semiconductors,* eds. R.K. Willardson and H.L. Goering (New York: Reinhold, 1962).
3. *Numerical Data and Functional Relationships in Science and Technology,* Vol. 17 of Landolt-Bornstein New Series (Berlin: Springer-Verlag).
4. M.B. Panish and M. Illegms, *Prog. Solid State Chem.* 7, 39 (1972); G.B. Stringfellow, *J. Cryst. Growth* 27, 21 (1976); 58, 194 (1982).
5. J.A. Van Vechten and T.K. Bergstresser, *Phys. Rev. B* 1, 3351 (1970).
6. J.E. Bernard and A. Zunger, *Phys. Rev. B* 36, 3199 (1987); 34, 5992 (1986).
7. S.-H. Wei and A. Zunger, *Phys. Rev. B* 39, 3279 (1989).
8. R. Magri, S. Froyen and A. Zunger, *Phys. Rev. B* 44, 7967 (1991); 43, 1662 (1991).
9. See M. Glicksman and W.D. Kraeft, *Solid-State Electron.* 28, 151 (1985) and references therein.
10. D. Vanderbilt and C. Lee, *Phys. Rev. B* 45, 11,192 (1992).
11. R. Osorio, S. Froyen, and A. Zunger, *Phys. Rev. B* 43, 14,055 (1991).
12. A. Aresti et al., *J. Electrochem. Soc.* 124, 766 (1977); J.N. Gan et al., *Phys. Rev. B* 13, 3610 (1976); L. Garbato and T. Ledda, *J. Solid State Chem.* 30, 189 (1979).
13. S.-H. Wei, L.G. Ferreira and A. Zunger, *Phys. Rev. B* 41, 8240 (1990); L.G. Ferreira, S.-H. Wei and A. Zunger, *Phys. Rev. B* 40, 3197 (1989); A. Mbaye, L.G. Ferreira and A. Zunger, *Phys. Rev. Lett.* 58, 49 (1987).
14. A. Sher, M. Van Schilfgaarde, A.B. Chen and W. Chen, *Phys. Rev. B* 36, 4279 (1987).
15. R. Osorio, Z.W. Lu, S.-H. Wei and A. Zunger, *Phys. Rev. B (in press);* K. Newman and X. Xiang, *Phys. Rev. B* 44, 4677 (1991).
16. M.J. Jou, Y.T. Cheng, H.R. Jen and G.B. Stringfellow, *Appl. Phys. Lett.* 52, 549 (1988).
17. J.E. Greene, *J. Vac. Sci. Technol. B* 1, 229 (1983).
18. D.M. Wood and A. Zunger, *Phys. Rev. B* 40, 4062 (1989); 38, 12,756 (1988); *Phys. Rev. Lett.* 61, 1501 (1988).
19. A. Zunger and D. M. Wood, *J. Cryst. Growth* 98, 1 (1989).
20. A. Mbaye, D.M. Wood and A. Zunger, *Phys. Rev. B* 37,3008 (1988); *Appl. Phys. Lett.* 49, 782 (1986).
21. K. Kim and E.A. Stern, *Phys. Rev. B* 32, 1019 (1988); L.C. Davis and H. Holloway, *Phys. Rev. B* 38, 4294 (1988).
22. C. Weisbuch and B. Vinter, *Quantum Semiconductor Structures* (New York: Academic Press, 1991).
23. G.H. Doehler, *Quantum Electr.,* QE 22, 1683 (1986).
24. (a) L. Esaki and R. Tsu, IBM, *J. Res. Develop.* 14, 62 (1970); (b) J.N. Schulman and T.C. McGill, *Appl. Phys. Lett.* 34, 663 (1979).
25. D.L. Smith, T.C. McGill and J.N. Schulman, *Appl. Phys. Lett.* 43, 180 (1983).
26. J. Reno and J.P. Faurie, *Appl. Phys. Lett.* 49, 409 (1986).
27. S.H. Wei and A. Zunger, *Appl. Phys. Lett.* 53, 2077 (1988).
28. R. Cingolani, L. Tapper and K. Ploog, *Appl. Phys. Lett.* 56, 1233 (1990).
29. M.A. Gell, D. Ninno, M. Jaros and D.C. Herbert, *Phys. Rev. B* 34, 2416 (1986).
30. D.B. Laks and A. Zunger, *Phys. Rev. B* 45, 11,411 (1992).
31. G.C. Osbourn, *J. Vac. Sci Technol. B* 2, 176 (1984).
32. S.R. Kurtz, G.C. Osburn, R.M. Biefield, L.R. Dawson and H.J. Stein., *Appl. Phys. Lett.* 52, 831 (1988).
33. R.G. Dandrea and A. Zunger, *Appl. Phys Lett.* 57, 1031 (1990).
34. T. Takarohashi and M. Ozeki, *Jpn. J. Appl. Phys.* 30, L956 (1991); *J. Cryst. Growth* 115, 538 (1991).
35. S. Froyen, D.M. Wood, and A. Zunger, *Phys. Rev. B* 36, 4547 (1987); 37, 6893 (1988); *Phys. Rev. Lett.* 62, 975 (1989); *Appl. Phys. Lett.* 54, 2435 (1989); *Thin Solid Films,* 183, 33 (1989).
36. See review by T.P. Pearsail, *Semiconductors and Semimetals,* 32 (New York: Academic Press, 1990), p. 1.
37. J.M. Gaines, P.M. Petroff, H. Kroemer, R.J. Simes, R.S. Gells and J.H. English *J. Vac Sci. Technol.* B6, 1378 (1988).
38. P.M. Petroff, A.C. Gossard and W. Wiegman, *Appl. Phys. Lett.* 45, 620 (1984).
39. T. Fukui and H. Saito, *J. Vac Sci. Technol.* B6, 1373 (1988).
40. K.C. Hsieh, J.N. Baillaryeon and K.Y. Cheng, *Appl. Phys. Lett.* 57, 2244 (1990); ibid 60, 2892 (1992); K.C. Hsieh, J.N. Baillaryeon, K.Y. Cheng, S. Bailey, C.H. Uri and M. Mochel, Mat. Res. Soc., xx, 263 (1990). See also P.M. Petroff, M. Tsuchiya and L.A. Coldren, *Surf. Sci.* 228, 24 (1990).
41. S.A. Chalmers, A.C. Gossard, P.M. Petroff, J.M. Gaines and H. Kroemer, *J. Vac. Sci. Technol.* B7, 1357 (1989).
42. S. Chalmers, A.C. Gossard and H. Kroemer, *J. Cryst. Growth* 111, 647 (1990).
43. M.S. Miller, H. Weman, C.E. Pryor, M. Krishnamurty, P.M. Petroff, H. Kroemer and J.L. Merz, *Phys. Rev. Lett.* 68, 3464 (1992).
44. K.Y. Cheng, K.C. Hsieh, J.N. Baillaryeon and A. Mascarenhas, *Inst. Phys. Conf. Ser.* 120, 589 (1991).
45. *Materials Issues in Micrystalline Semiconductors,* eds. P.M. Fauchet, K. Tanaka and C.C. Tsai (Pittsburgh, PA: Materials Research Society, 1990).
46. (a) W.M. Meier and D.H. Olson, *Atlas of Zeolite Structure Types,* 3rd Ed. (Guildford, Eng.: Butterworth, 1992). G.D. Stucky, E. Ramli, D. Margolese, P. Petroff, S. Tomiya, J. Nicol, C. Glinka, J. Rush, *Nanophase and Nanocomposite Materials* (Pittsburgh, PA: Materials Research Society, to be published in 1993); R.K. Iler, *The Chemistry of Silica* (New York: J. Wiley and Sons, 1979); D. Vaughn and R.J. Lussier, *Proc. 5th Intern. Conf on Zeolites* (L. V. C. Rees ed. Hyden), 94 (1980); W.M. Meier, *New Developments in Zeolite Science and Technology,* Stud. Surf. Sci. Catal., 13, eds. Y. Murakami, A. Ijima, and J. W. Ward (New York: Elsevier Science) 28 (1986).
(b) S. Tomiya, P.M. Petroff, D. Margolese, V. Srdanovand and G. Stucky, *Nanophase and Nanocomposite Materials* (Pittsburgh, PA: Materials Research Society, to be published in 1993).
47. F. Gutmann and L.E. Lyons, *Organic Semiconductors* (New York: Wiley, 1967).
48. D.L. Morel et al., *Conf. Rec. 10th IEEE Photovoltaic Specialists Conf.* (New York: IEEE, 1974), p. 107.
49. F.F. So and S.R. Forrest, *Phys. Rev. Lett.* 66, 2649 (1991).
50. A. Zunger, *Appl. Phys. Lett.* 50 (1987), p. 164.
51. J. Bernard, S.H. Wei, D.M. Wood and A. Zunger, *Appl. Phys. Lett.* 52, 311 (1987); S.-H. Wei and A. Zunger, *Appl. Phys. Lett.* 56, 662 (1990).
52. R. Osorio, E. Bernard, S. Froyen and A. Zunger, *Phys. Rev. B* 45, 11,173 (1992).
53. T. Suzuki et al., *Jpn. J. Appl. Phys.* 27, 2098 (1988); T. Nishino et al., *Appl. Phys. Lett.* 53, 583 (1988).
54. S.-H. Wei and A. Zunger, *Appl. Phys. Lett.* 58, 2684 (1991) and unpublished results.
55. S.R. Kurtz, L.R. Dawson, R.M. Biefeld, D.M. Follstaedt and B.L. Doyle, *Phys. Rev. B* 46, 1909 (1992).
56. D.M. Wood and A. Zunger, *Phys. Rev B* 34, 4105 (1986).
57. A.E. Carlson, D.M. Wood and A. Zunger, *Phys. Rev. B* 32, 1386 (1985); S.H. Wei and A. Zunger, *Phys. Rev. Lett.* 56, 528 (1986); D.M. Wood, A. Zunger and R. de Groot, *Phys. Rev. B* 31, 2570 (1985); N.E. Christensen, *Phys. Rev. B* 32, 6490 (1985).
58. K. Kuriyama and F. Nakamura, *Phys Rev. B* 36, 4439 (1987); *Appl. Phys. Lett.* 69, 7812 (1991); R. Bacewicz and T.F. Ciszek, *Appl. Phys. Lett.* 52, 1150 (1988); A. Nelson, M. Engelhardt and M. Hochst, *J. Elect. Spect.* 51, 623 (1990).
59. J.L. Shay and J.H. Wernicke, *Ternary Chalcopyrites* (Oxford, U.K.: Pergamon Press, 1975).
60. J.L. Martins and A. Zunger, *Phys. Rev. B* 32, 2689 (1985).
61. J. Jaffe and A. Zunger, *Phys. Rev. B* 27, 5176 (1983); 28, 5822 (1983); 30, 741 (1984).
62. J.E. Jaffe and A. Zunger, *Phys. Rev. B* 29, 1882 (1984).
63. E. Parthé, *Crystal Chemistry of Tetrahedral Structures* (New York: Gordon & Breach, 1964).
64. J.E. Bernard and A. Zunger, *Phys. Rev. B* 37, 6835 (1988).

65. E. Bucher, *Photoelectrochemistry and Photovoltaics of Layered Semiconductors,* ed. A. Aruchamy (Amsterdam, the Netherlands: Kluwer, 1991).
66. F. Gutmann, *Modern Bioelectrochemistry,* eds. F. Guttmann and H. Keyzer (New York: Plenum, 1986), pp. 177–197.
67. R. Pethig, ibidem, pp. 199–231.
68. R.R. Birge et al., *Nonlinear Electrodynamics in Biological Systems,* eds. W.R. Adey and A.F. Lawrence (New York: Plenum, New York, 1984), pp. 107–120.

REFERENCES FOR TABLE I

a. A. Ooe and S. Iida, *Jpn. J. Appl. Phys.* 29, 1484 (1990).
b. V.G. Lambrecht, *Mat. Res. Bull.* 8, 1383 (1973).
c. L. Garbato, F. Ledda and P. Manca, *Jpn. J. Appl. Phys.,* Suppl., 19-3, 67 (1980).
d. A. Aresti et al., *J. Electrochem. Soc* 124, 766 (1977).
e. J.N. Gan et al., *Phys. Rev. B,* 12, 5797 (1975); ibid, 13, 3610 (1976).
f. D. Chippaux and A. Deschanvres, *J. Solid State Chem.* 45, 200 (1982).
g. W. Gebicki, M. Igalson and R. Trykozko, *Acta Phys. Pol. A* 77, 367 (1990).
h. L. Garbato and F. Ledda, *J. Solid State Chem.* 30, 189 (1979).
i. C. Neal et al., *J. Phys. D* 22, 1347 (1989).
j. R. Tovar et al., *J. Cryst. Growth* 106, 629 (1990).
k. M. Quintero et al., *J. Solid State Chem.* 63, 110 (1986).
l. M. Quintero et al., *J. Solid State Chem.* 87, 456 (1990).
m. R. Tovar et al., *Phys. Status Solidi A* 111, 405 (1989).
n. M. Quintero and J. C. Wooley, *Phys. Status Solidi A* 92, 449 (1985).
o. F. Grima et al., *Phys. Status Solidi A* 107, 165 (1988).

REFERENCES FOR TABLE II

a. M.A.E. Maslout and C. Gleitzer, *Compt. Rendus.* 271 Ser C, 1177 (1970).
b. R. Juza and F. Hund, *Naterwiss* 33, 121 (1946); Z. Anorg, *Allg. Chem.* 257, 1 (1948).
c. H. Nowotny and K. Bachmayer, *Monatshafte. Chem.* 81, 488 (1950); ibid 80, 735 (1949).
d. F. Laves, *Taschbenbuch für Chemiker und Physiker,* eds. J. D'Ans and E. Lax (Berlin, Germany: Springer-Verlag, 1943).
e. R. Juza, W. Dethlefsen, H. Seidel and K. Benda, *Z. Anorg. Allg. Chem.,* 356, 253 (1968); R. Juza, K. Langes and K Benda, *Anorg, Chem. Intnt. Edition,* 7, 360 (1968).
f. M.A. El Maslout, J.P. Motte, C. Gleitzer and J. Aubry, *Compt. Rendus.* 273, Ser. C, 707 (1971).
g. H. Nowotny et al., *Monatshafte. Chem.* 82, 720 (1951).
h. W.B. Pearson, *Handbook of Lattice Spacings and Structure of Metals and Alloys* (New York: Pergamon Press, 1958), Vol. 1, p. 400 describes NaHgAs as FCC, cubic, Cl Type Structure. See also H. Nowotny, *Holub, Monatshafte Chem.* 91, 877 (1960).
i. H. Nowotny and W. Sibert, *Z. Metallkd.* 33, 391 (1941).
j. H. Nowotny, *Metallforsch* 1, 138 (1946).
k. H. Nowotny, *Z. Metallkd.* 7, 273 (1942).